Monthly Notices
of the
ROYAL ASTRONOMICAL SOCIETY

Mon. Not. R. Astron. Soc. **404,** 1349–1354 (2010) doi:10.1111/j.1365-2966.2010.16391.x

The dependence of the properties of optical fibres on length

C. L. Poppett★ and J. R. Allington-Smith★

Centre for Advanced Instrumentation (CfAI), Durham University, South Road, Durham DH1 3LE

Accepted 2010 January 20. Received 2010 January 20; in original form 2010 January 8

ABSTRACT

We investigate the dependence on length of optical fibres used in astronomy, especially the focal ratio degradation (FRD) which places constraints on the performance of fibre-fed spectrographs used for multiplexed spectroscopy. To this end, we present a modified version of the FRD model proposed by Carrasco & Parry to quantify the number of scattering defects within an optical fibre using a single parameter. The model predicts many trends which are seen experimentally, for example, a decrease in FRD as core diameter increases, and also as wavelength increases. However, the model also predicts a strong dependence on FRD with length that is not seen experimentally. By adapting the single fibre model to include a second fibre, we can quantify the amount of FRD due to stress caused by the method of termination. By fitting the model to experimental data, we find that polishing the fibre causes more stress to be induced in the end of the fibre compared to a simple cleave technique. We estimate that the number of scattering defects caused by polishing is approximately double that produced by cleaving. By placing limits on the end effect, the model can be used to estimate the residual-length dependence in very long fibres, such as those required for Extremely Large Telescopes, without having to carry out costly experiments. We also use our data to compare different methods of fibre termination.

Key words: instrumentation: spectrographs – techniques: spectroscopic – methods: laboratory.

1 INTRODUCTION

Focal ratio degradation (FRD) is the non-conservation of étendue in an optical fibre, resulting in a broadening of the beam at the output. As noted by Parry (2006), an increase in étendue within the instrument without a gain in information content is undesirable because the optical system which has to deal with it is consequently more complex and expensive. As telescopes increase in size, the large optical path lengths caused by the remoteness of focal stations from gravitationally invariant instrument platforms and the increased sensitivity to mechanical flexure, mean that optical fibres will continue to be important for the key technique of highly multiplexed spectroscopy (Allington-Smith 2007). Therefore, it is even more important to be able to predict the performance of optical fibres accurately in order to optimize the instrument system performance.

In this paper, we propose a modification to a model first proposed by Gloge (1972) and later adapted by Gambling, Payne & Matsumura (1975) and Carrasco & Parry (1994). The model is described in Section 2.1. This modification aims to eliminate the dependence on FRD with length which is predicted theoretically but not seen experimentally. By modelling the fibre as two separate fibres with different amounts of scattering defects, it can be shown that most of the FRD is caused by the stress frozen in at the fibre ends during end preparation.

The need for the fibre ends to be flat, smooth and perpendicular to the axis of the fibre is well documented, although the method of end preparation varies widely depending on various restrictions. The quickest way to prepare a fibre is cleaving, typically by scoring it with a diamond pen or tungsten-carbide-edged blade, although a CO_2 laser (Kinoshita & Kobayashi 1979) or spark erosion (Caspers & Neumann 1976) has also been used. Once the fibre has been scored, it is placed under tension and then bent along the fracture until it snaps. Although this method is relatively quick to perform, the results are not always satisfactory and a visual inspection must be performed. In addition to the problem of repeatability, it is extremely difficult to avoid a small defect occurring at the point where the fibre is scored as is shown in panel (a) of Fig. 1. The second method is to polish the fibre on progressively finer grades of abrasive paper and finally on a solution of colloidal silica. This method of polishing the fibre is time consuming, however visual and interferometric inspection of the end normally shows it to be high quality. Haynes (2008) have shown that the quality of the polish has a large effect on the FRD by comparing fibres with end face roughness of 245 and 6 nm rms.

Fig. 1 shows the typical finish which can be expected when a fibre is cleaved or polished. However, all methods of preparing the ends of the fibre produce stress. The amount of stress and the depth to which

★E-mail: c.l.poppett@durham.ac.uk (CLP); j.r.allington-smith@durham.ac.uk (JRAS)

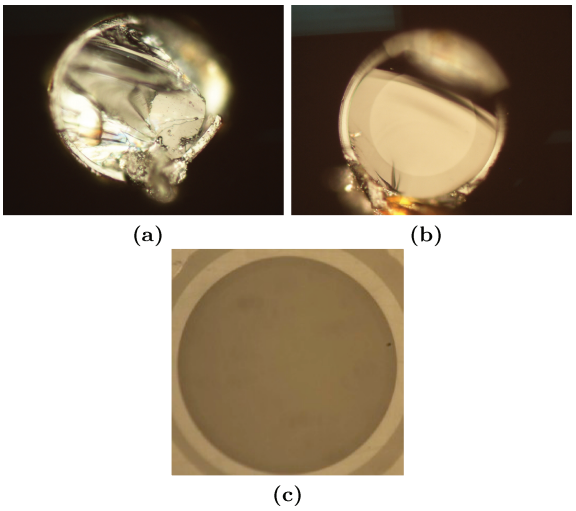

Figure 1. Results of different methods of end preparation for a typical fibre with a diameter of 100 μm (a) unprepared (b) after cleaving (c) after polishing. In panel (b), the defect from scoring the fibre is clearly visible.

it propagates from the end face is currently impossible to measure, and methods can only be compared based on the smoothness of the finish as assessed with a microscope or interferometer. The most common rule of thumb is that stress propagates to 3 times the depth of the biggest defect on the end face of the fibre although this has never been proven. It has been shown by Craig, Hailey & Brodie (1988) that for the various fibres that they tested, there is no observable difference in FRD between a properly cleaved fibre and a polished fibre.

In Section 2.2, we modify the Gloge model to include two fibres with different properties in series. This allows us to model the end effect as a short fibre of fixed length with a larger number of scattering defects per unit length, d_0, than the main length of fibre. This parameter, d_0 has different values depending on the termination method used.

It has been shown by Avila et al. (1988) that FRD is strongly affected by the way in which a fibre is mounted. Avila et al. tested ultraviolet grade silica fibres and found that, at an input focal ratio of $F_{\rm in} = 8$, $F_{\rm out}$ fell from $F/6.2$ when the fibre was held gently in a clamp to $F/3.2$ when it was squeezed strongly. This is an important issue because fibres are usually mounted in a ferrule or holder to protect the tip and allow them to be polished in bulk. When the fibres are mounted in this way they must be glued into position, and it is extremely important to test the effects of various adhesives on the resultant FRD as shown by Oliveira, Oliveira & dos Santos (2005). This model also provides a quantitative measure of these mounting methods which will be independent of the fibre used.

2 THEORY

2.1 Gloge's model

Carrasco & Parry (1994) have shown that it is possible to measure the FRD of an optical fibre and characterize its performance using a single parameter, D. The model is based on a previous model by Gloge (1972) who showed that the far-field distribution represents a direct image of the modal power distribution. Gloge developed a partial differential equation to describe the distribution of optical power P in a fibre of length L in terms of the axial angle of incidence $\theta_{\rm in}$, with output angle $\theta_{\rm out}$.

$$\frac{\partial P(\theta_{\rm out}, \theta_{\rm in})}{\partial L} = -A\theta_{\rm in}^2 P(\theta_{\rm out}, \theta_{\rm in}) + \frac{D}{\theta_{\rm in}} \frac{\partial}{\partial \theta_{\rm in}} \left[\theta \frac{\partial P(\theta_{\rm out}, \theta_{\rm in})}{\partial \theta_{\rm in}} \right], \tag{1}$$

where A is an absorption coefficient and D is a parameter that depends on the constant d_0 that characterizes microbending,

$$D = \left(\frac{\lambda}{2 d_{\rm f} n} \right)^2 d_0, \tag{2}$$

λ is the wavelength of light, $d_{\rm f}$ the fibre core diameter and n the index of refraction of the core. Equation (1) has been solved by Gambling et al. (1975) for the case of a collimated input beam of angle of incidence $\theta_{\rm in}$,

$$P(\theta_{\rm out}, \theta_{\rm in}) = \exp\left\{ -\left(\frac{\chi_i + \chi}{2} \right) \left[\frac{1 + \exp(-bL)}{1 - \exp(-bL)} \right] \right\} \times \left[\frac{\exp(-bL/2)}{1 - \exp(-bL)} \right] I_o \left[\frac{(4\chi_i \chi)^{1/2} \exp(-bL/2)}{1 - \exp(-bL)} \right], \tag{3}$$

where $\chi = (A/D)^{1/2}\theta_{\rm in}^2$, $b = 4(AD)^{1/2}$, and I_0 is the modified Bessel function of zeroth order.

Equation (3) describes the angular dependence on the output flux in the far field for the case of a collimated input beam at an angle of incidence $\theta_{\rm in}$. It is possible to generalize the solution given by equation (3) to the case of an input beam with any aperture as follows:

$$F(\theta_{\rm out}, \theta_0) = \int_0^{2\pi} \int_0^{\pi} G(\theta_{\rm in}, \phi, \theta_0) P(\theta_{\rm out}, \theta_{\rm in}) \sin\theta_{\rm in} {\rm d}\theta_{\rm in} {\rm d}\phi, \tag{4}$$

where $\sin\theta_{\rm in} {\rm d}\theta_{\rm in} {\rm d}\phi = {\rm d}\Omega$ is the differential of solid angle, ϕ is the azimuthal angle measured around the same axis, and G is a function that represents the input beam.

Carrasco & Parry have shown that when the value of D is found for a specific fibre, the results of other experiments where the far field output beam is recorded for input pencil beams of varying focal ratio, can be successfully predicted. By testing a 200 μm core fibre Carrasco and Parry found a solution to D which produced a reasonable fit to the experimental data. From their data, the accuracy of optical alignment can be inferred to be 1° since this shifts the predicted output focal ratio by 2.5 per cent which is the typical size of their experimental errors.

As shown by equation (2), the D parameter depends on the fibre core diameter, $d_{\rm f}$, the microbending parameter, d_0, the wavelength of the injected light, λ, and the length of the fibre, L. From this equation, it is clear the $D \propto \lambda^2$, and hence FRD will increase as the wavelength increases. This result has been verified experimentally (Poppett & Allington-Smith 2007), although the opposite trend has been reported by Murphy et al. (2008), who found a weak dependence on FRD with wavelength. However, measurements were made at $F_{\rm in} = 3.5$, where FRD is relatively unimportant compared to slower beams where the output beam approaches an asymptotic value.

FRD be quantified conveniently by the FRD ratio $F_{\rm in}/F_{\rm out}$. The second trend predicted by equation (2) is that $D \propto d_{\rm f}^{-1}$. Fig. 2 shows how this model and the two-fibre model described in Section 2.2, predict how different parameters will affect the resulting output power distributions.

Whilst the trends shown for the fibre core and d_0 parameter dependence have been demonstrated experimentally as well as theoretically, the extent to which the length affects the FRD has not. Gambling et al. did report a length dependence, however this result was for liquid-core fibres. This result has never been reproduced

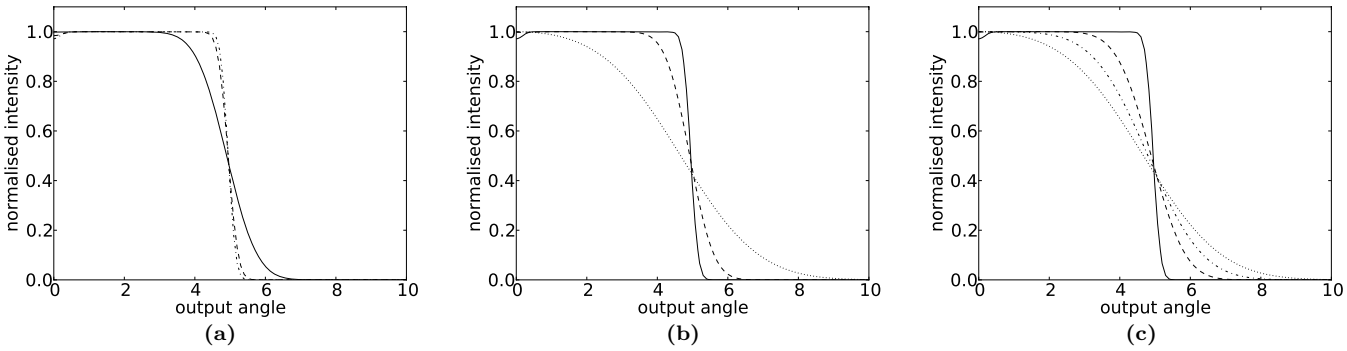

Figure 2. Normalized theoretical results to show how the output power distribution will be affected by changing the input parameters. All results are for a solid input beam of angle 5° and unless otherwise stated for a fibre of length 1 m, $d_f = 100$ μm, and $d_0 = 1$. (a) $d_f = 25$ μm (solid), 75 μm (dashed), 100 μm (dot–dashed); (b) $d_0 = 1$ (solid), 20 (dashed), 50 (dot–dashed), 100 (dotted); (c) $L = 1$ m (solid), 10 m (dashed), 100 m (dot–dashed).

for monolithic fused silica fibres. To confirm this assumption, an experiment was set up as described in Section 3. The following section gives the theoretical description of the method of eliminating this length dependence.

2.2 The two-fibre model

In order to add a second fibre into the model it is assumed that for a single input ray at angle θ_{in} to the fibre axis, the output surface brightness at angle θ_{out} is given by the Gloge model as $F(\theta_{out}, \theta_{in})$.

For a solid input angle defined by unit surface brightness for $\theta_{in} < \theta_0$, the total output surface brightness is given by

$$F_1(\theta_{out,1}, \theta_0) = \int_0^{\theta_0} F(\theta_{out,1}, \theta_{in,1}) 2\pi\theta_{in,1} \mathrm{d}\theta_{in,1}. \quad (5)$$

If a second fibre is added to receive light from the first fibre, the equivalent number of single rays it sees at the input is given by

$$\mathrm{d}N(\theta_{out,1}) \propto F_1(\theta_{out,1}, \theta_0) 2\pi\theta_{out,1} \mathrm{d}\theta_{out,1}, \quad (6)$$

so the output surface brightness in terms of the angle at the exit of the second fibre, $\theta_{out,2}$, is

$$\begin{aligned} F_2(\theta_{out,2}, \theta_0) &= \int_0^{\infty} F(\theta_{out,2}, \theta_{out,1}) \mathrm{d}N(\theta_{in,2}) \\ &= \int_0^{\infty} F(\theta_{out,2}, \theta_{out,1}) F_1(\theta_{out,1}, \theta_0) \\ &\quad \times 2\pi\theta_{out,1} \mathrm{d}\theta_{out,1}. \end{aligned} \quad (7)$$

The coupling between fibres is achieved by setting $\theta_{in,2} = \theta_{out,1}$.

Fig. 3 shows curves for the output power distribution produced by both the one-fibre and two-fibre model. Since we cannot determine $d_{0,2}$ and L_2 independently, we use the product $S = d_{0,2}L_2$ to characterize the second fibre. This parameter essentially quantifies the total number of scattering centres (microbends) present in the second fibre. The value of S was chosen to produce the same amount of FRD at the asymptotic value as the one-fibre model. This figure shows that the two-fibre model agrees well with the predictions made by the one-fibre model (itself rigorously tested against experimental data here and elsewhere). Indeed the difference in the 95 per cent enclosed energy values of the one- and two-fibre models differ by the same amount as the experimental error bars (see below). We use the angle which encloses 95 per cent of the energy to define the output focal ratio since this reduces sensitivity to stray light in the experimental setup.

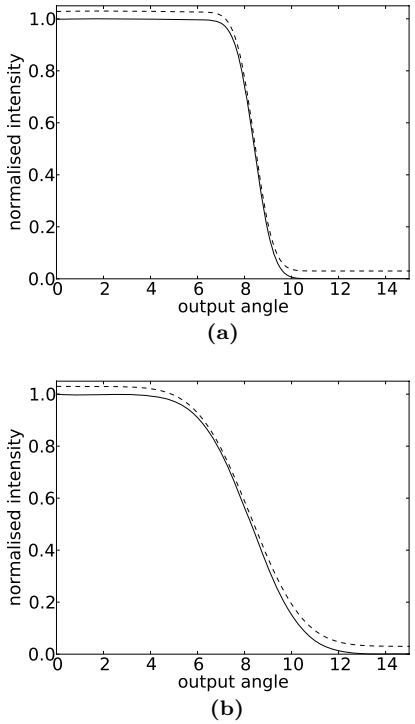

Figure 3. Output power distributions predicted by the one fibre (dashed) and two fibre models (solid, with an offset of 0.03 in order to be able to show both curves).

3 EXPERIMENTAL RESULTS

To test the experimental dependence on FRD with length, a fibre was illuminated with a solid input beam of varying θ_{in} as shown by Fig. 4. The fibre used was a typical fibre made by polymicro (FIP100110125) with a core diameter of 100 μm, which has similar characteristics to fibres used in astronomical instruments. Input beams ranging between f/1.7 and f/18.9 (i.e. cone half-angles 16°–1.5°) were used to investigate how the FRD evolved with input angle.

Tests were taken for a case of a cleaved fibre of length 10 m immersed via index-matching gel to a smooth flat glass plate and for the same fibre after it had been polished to a 1 μm optical finish. The FRD curve presented in Fig. 5 shows that the fibre has a fairly good FRD performance with an FRD ratio of around 1.1 at $F_{in} = 4.5$. The rationale for testing a cleaved fibre with index matching gel was

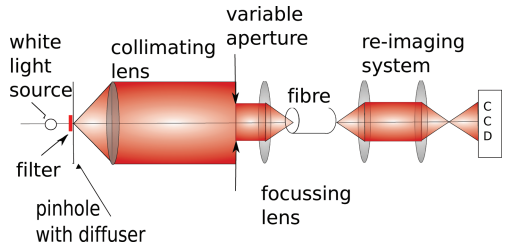

Figure 4. Experimental setup. The adjustable iris was used to give a range of input focal ratios and a beam splitter was used in order to provide an image of the input light on the end face of the fibre.

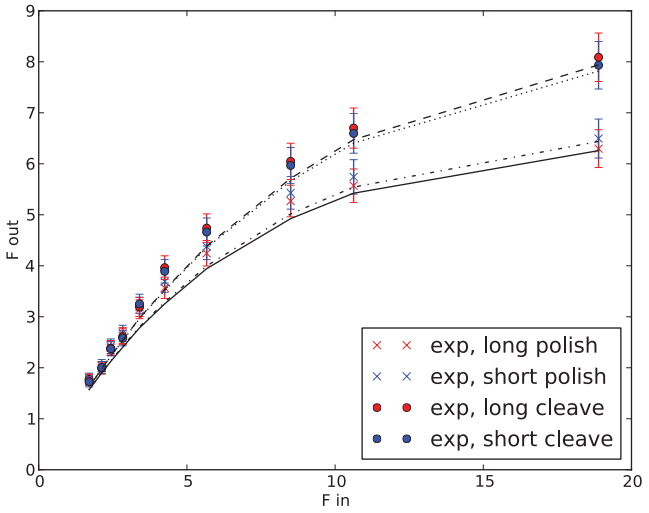

Figure 5. FRD curves where experimental results are shown by crosses and theoretical results produced by the original one-fibre model are given by a smooth line.

Table 1. Parameters need to produce theoretical curves which match experimental results for the fibre preparation methods.

Preparation method	Fibre length	FRD ratio (at $F_{in} = 4.5$)	d_0 (m^{-1})	D (m^{-1})
Cleave	Long	1.07	5.0	2.1×10^{-5}
Cleave	Short	1.09	52	2×10^{-4}
Polish	Long	1.19	9.1	4×10^{-5}
Polish	Short	1.15	85	3.7×10^{-4}

to make sure that we isolated the effect of stress from any scattering caused by imperfections in the topography of the end face. The use of index-matching gel for the cleaved fibre should eliminate the effect of surface roughness and the smoothness of the finish would do the same for the polished fibre. Furthermore, we expected that cleaving would result in relatively low stress and therefore provide a baseline against which the results of the polishing could be compared.

The test was repeated after the fibre had been cut to a length of 1 m for both the cleaved polished case. These two lengths of fibre will be referred to as 'long' and 'short' for the remainder of this report.

The measured FRD for all scenarios under which the fibre was tested are also shown in Fig. 5. From this, the D parameter for the fibre has been estimated in each of the specific cases (Table 1). Theoretical predictions using these parameters are shown in Fig. 5. From this, we estimate that the difference in FRD due to the different fibre lengths for the cleaved fibre at the asymptotic value was 0.15 ± 0.7, and hence is clear that within our experimental uncertainty, no length dependence is observed.

4 DISCUSSION OF RESULTS

We now use the experimental results to eliminate the length dependency and compare stress induced by different end preparation techniques. To this end, the model can be run for various combinations of $d_{0,1}$ and S (where $S = d_{0,2}L_2$) to find a single set of values which predict the experimentally observed FRD curves. In order to find this set of values, a number of constraints can be applied to the two-fibre model, such that we require:

(i) $d_{0,1}$, S combinations where the difference in asymptotic F_{out} for the long and short fibres is less than the experimental errors;
(ii) $d_{0,1}$, S combinations which give an F_{out} which agrees with the experimental data at the asymptote for both the cleaved and polished fibres;
(iii) $d_{0,1}$ value less than that determined from the one-fibre model, and the same for both the cleaved and polished fibres.

As is shown in Section 3, the length dependence was less than $F/0.15 \pm 0.67$ for the cleaved fibre. The contour plot shown in panel (a) of Fig. 6 defines the upper limit on allowable ΔF, and all values within the 0.7 contour region give acceptable solutions for specific values of $d_{0,1}$ and S. Secondly, the asymptotic F_{out} must be the same as the experimental data within the error bars. For the case of the cleaved fibre, the error in F_{out} was determined to be 0.46 and this contour is shown in panel (b) of Fig. 6. All values within this 0.46 contour region give acceptable solutions for specific $d_{0,1}$ and S. The final panel in Fig. 6 shows how these constraints combine, and a solution for the cleaved fibre is shown by a cross at $d_{0,1} = 0.1\ m^{-1}$ and $S = 25$. Using these constraints for the polished fibre produces a solution at $d_{0,1} = 0.1\ m^{-1}$ and $S = 48$.

Fig. 7 shows the FRD curves for various lengths of fibre using these parameters. From this figure, it is clear that we have removed the length dependence of the model within the lengths for which it was constrained. The small discrepancies between the theoretical and experimental results arise due to misalignments within the experiment and the fact that we have assumed G was a perfect step function rather than measuring it explicitly.

The second objective of the two-fibre model is to provide a method of comparing stress induced by various end preparation techniques. Comparison of the parameter, S, between the polished and cleaved cases gives a quantitative assessment of the induced stress. The relative values show that there are twice as many microbends per unit length when polishing the fibre, compared to when it is cleaved. The high absolute values of S make a very strong argument for taking great care to eliminate stress in the end-preparation process.

Currently, there is no method of determining the depth to which stress in the end of the fibre extends. The rule of thumb that the stress propagates to 3 times the depth of the largest defect on the end face of the fibre implies that the stress only affects a few μm of the length of the fibre and forces $d_{0,2}$ to be extremely large. Thus, assuming that the defect size is determined by the smallest grit size, implies $L_2 = 3\ \mu m$ and $d_{0,2} = 8.3 \times 10^6\ m^{-1}$ and $d_{0,2} = 16.0 \times 10^6\ m^{-1}$ for the polished and cleaved fibres, respectively.

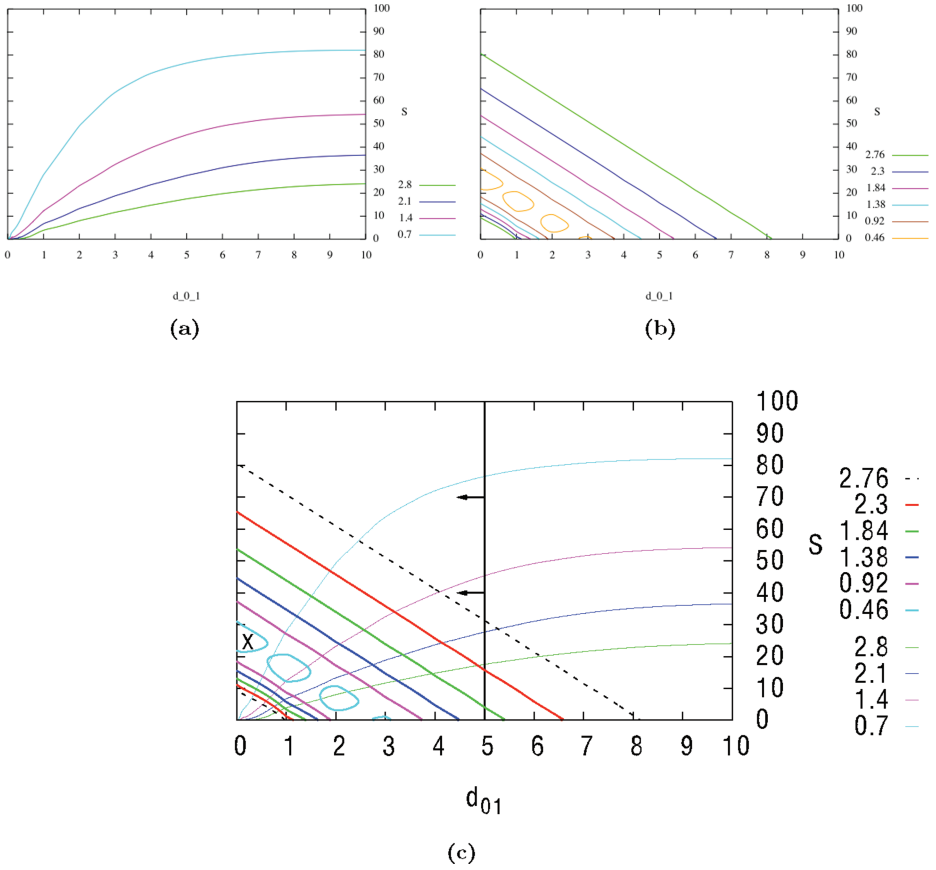

Figure 6. The two fibre model was run for various combinations of $d_{0,1}$ and S (where $S = d_{0,2}L_2$). Panel (a) shows the difference in asymptotic F_{out} between $L = 1$ and $L = 10$ m with contours shown in increments of 0.7. Panel (b) shows the difference in asymptotic F_{out} between experimental and theoretical results for the cleaved fibre. Panel (c) shows how these graphs can be combined to find a single solution, marked by the large cross, for $d_{0,1}$ and S which satisfies experimental data. The black vertical line in panel (c) shows the $d_{0,1}$ parameter predicted by the one-fibre model for the cleaved fibre.

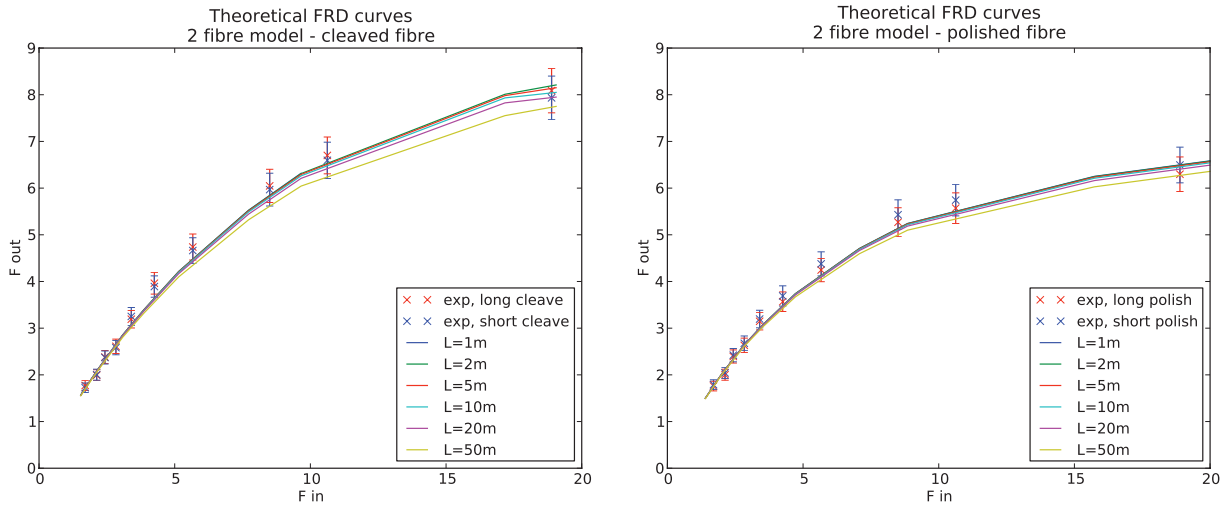

Figure 7. Two-fibre model results with $d_{0,1} = 0.1\ \text{m}^{-1}$ and $d_{0,2}L_2 = 25$ for the cleaved fibre and $d_{0,2}L_2 = 48$ for the polished fibre. It is clear that within the errors the length dependence of the original model has been removed.

5 CONCLUSIONS

We have adapted the power distribution model described by Gloge and produced a new model which will eliminate the length dependence on FRD in order to provide a better agreement with experimental data. This model has been tested against the original one-fibre model, and with experimental data, and shown to be in good agreement. As a result of trying to quantify the amount of stress within the end of the fibre it has been shown that the end effect is extremely powerful. If we assume that the $d_{0,2}$ parameter characterizes the FRD induced in the end of the fibre then it is possible to compare how the FRD produced in the majority of the

length of the fibre is affected. In the case of the cleaved fibre, the d_0 parameter (which quantifies the amount of microbending) calculated using the one fibre model was reduced from $5\,m^{-1}$ for a 1-m fibre and $52\,m^{-1}$ for a 10 m fibre to $0.1\,m^{-1}$ independent of length using the two-fibre model. This significant reduction is testament to the strength of the end effect and clearly shows how much FRD is generated in the end of the fibre.

It was initially assumed that cleaving the fibre would produce very little stress, however this was not shown to be the case. This model is therefore extremely useful when comparing various end preparation techniques. For example, our results show that cleaving the fibre halves the strength of the end effect compared with polishing. The model can also provide an upper limit on the FRD performance of any length of fibre, and will therefore prove to be very useful when building instruments for Extremely Large Telescopes.

REFERENCES

Allington-Smith J. R., 2007, MNRAS, 376, 1099
Avila G., 1988, in Barden S. C., ed., ASP Conf. Ser. Vol. 3, Fiber Optics in Astronomy. Astron. Soc. Pac., San Francisco, p. 63
Carrasco E., Parry I. R., 1994, MNRAS, 271, 1
Caspers Fr., Neumann R. G., 1976, Electronics Lett., 12, 443
Craig W. W., Hailey C. J., Brodie J. P., 1988, in Barden S. C., ed., ASP Conf. Ser. Vol. 3, Fiber Optics in Astronomy. Astron. Soc. Pac., San Francisco, p. 41
Gambling W. A., Payne D. N., Matsumura H., 1975, Applied Optics, 14, 1538
Gloge D., 1972, Bell Syst. Tech. J., 51, 1767
Haynes D., 2008, in Atad-Ettedgui E., Lemke D., eds, Proc. SPIE Vol. 7018, Advanced Optical and Mechanical Technologies in Telescopes and Instrumentation. SPIE, Bellingham, p. 70182
Kinoshita K., Kobayashi M., 1979, Applied Opt., 18, 3256
Murphy J. D., MacQueen P. J., Hill G. J., Grupp F., Kelz A., Palunas P., Roth M., Fry A., 2008, in Atad-Ettedgui E., Lemke D., eds, Proc. SPIE Vol. 7018, Advanced Optical and Mechanical Technologies in Telescopes and Instrumentation. SPIE, Bellingham, p. 104
Oliveira A. C., Oliveira L. S., dos Santos J. B., 2005, MNRAS, 356, 1079
Parry I., 2006, New Astron. Rev., 50, 304
Poppett C. L., Allington-Smith J. R., 2007, MNRAS, 356, 1079

This paper has been typeset from a TEX/LATEX file prepared by the author.